Free Radical Biology & Medicine, Vol. 35, No. 9, pp. 1129–1137, 2003

0891-5849/03/$–see front matter

doi:10.1016/S0891-5849(03)00495-7

Original Contribution

ANTIOXIDANT CAPACITY OF SILICA HYDRIDE: A COMBINATIONAL PHOTOSENSITIZATION AND FLUORESCENCE DETECTION ASSAY

CORY J. STEPHANSON and G. PATRICK FLANAGAN
Flantech Group, Watsonville, CA, USA

(*Received* 24 *April* 2003; *Revised* 27 *June* 2003; *Accepted* 24 *July* 2003)

Abstract—Utilizing a novel combinational technique incorporating spectrafluorometry and photosensitization, this analysis determined cell viability and cytotoxicity through the introduction of reactive oxygen species and measurement of plasma membrane integrity. Chinese hamster ovary and mouse hybridoma cells were treated with silica hydride after being photosensitized with singlet oxygen, hydroxyl/superoxide, and hydroxyl reactive oxygen species through the use of rose Bengal diacetate, malachite green, and N,N′-bis(2-hydroperoxy-2-methoxyethyl)-1,4,5,8-naphthaldiimide, respectively. The analysis resulted in an easy and effective method for quantifying reactive oxygen species reduction and characterized the radical reduction efficacy of silica hydride at 97% (± 0.68%, $\sigma = 0.84$) against singlet oxygen species and over 87% (± 0.56%, $\sigma = 0.70$) for the combination of hydroxyl and superoxide reactive species, and 98% (± 0.37%, $\sigma = 0.47$) effective for hydroxyl radical species. Nontreated photosensitized controls showed less than 1% viability under the same conditions. © 2003 Elsevier Inc.

Keywords—Oxygen, Free radicals, Photosensitization, Silica, Hydride, Fluorescence, Antioxidant

INTRODUCTION

Biomolecular reactions with free radicals and their relationship with oxidative stress has been the subject of a multitude of scientific investigations and consistently tops the list of current topics in health and medicine. Reactive oxygen species (ROS) [1,2] have been shown to be integral in the causation of numerous cellular anomalies, including protein damage, deactivation of enzymatic activity, alteration of DNA and lipid peroxidation of membranes [3,4]. When the ROS accumulation exceeds the limits of what the natural cellular antioxidant effects can neutralize and deem inert, numerous pathological effects may manifest in the cells, including atherosclerosis, senescence, carcinogenesis, reperfusion injury, rheumatoid arthritis, and various blood disorders [5,6]. Additionally, this oxidative stress has been directly linked to dysfunctions and diseases include cardiomyopathy, diabetes, porphyria, halogenated liver injury, adriamycin cardiotoxicity, segmental progeria disorders, cataractogenesis, and multiple sclerosis [7–9]. It has become evident over the last decade that ROS-induced pathologies are of a serious and significant nature. Due to the significant pathological implications of oxidative stress, it is biochemically important to find a specific scavenger to efficiently and effectively reduce multiple ROS [10,11].

In vitro radical scavenging assays have traditionally been performed by utilizing radical-inhibiting chemiluminescence, a scavenger-specific fluorometric analysis, or by additional techniques such as electron spin resonance (ESR) spectroscopy. This is generally accomplished with the introduction of the ROS through a Fenton or EDTA- type reaction [12,13]. Although these methods of analysis are well established, they may not be optimally suited for biological analysis due to reactive interference of the chemical reagents and may not be suitable as an accurate representation of biological environments and pH ranges.

This assay used a series of simple techniques in fluorometric and photosensitization analysis to test the efficacy of a recently described compound, silica hydride [14]. Silica hydride (Fig. 1) is a novel, organosiliceous colloid that has interstitially embedded hydride anions. The compound is synthesized though the exposure of a silsesquioxane monomer (or other silicate substrate) in a

Address correspondence to: Dr. G. Patrick Flanagan, 195 Aviation Way, Watsonville, CA 95076, USA; Tel: (831) 406-0134; Fax: (831) 786-8903; E-Mail: patrick@flantech.com.

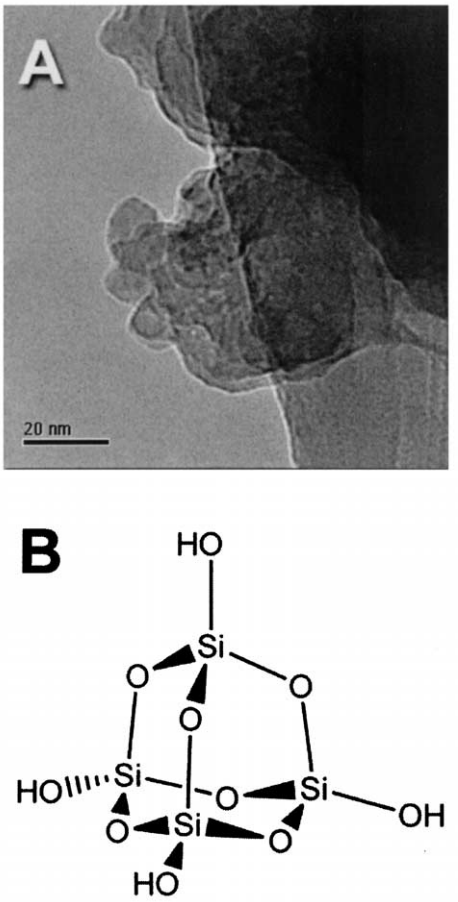

Fig. 1. A scanning transmission electron micrograph (STEM) image of the silica hydride compound (A), as taken by a Phillips CM30 STEM illustrates the small organosiliceous spheres that act as colloidal carriers for the hydride anions of silica hydride. The simple drawing of silica hydride (B) illustrates the silsesquioxane, caged-structure that the hydride anions are interstitially embedded into through a plasma-generated reaction.

pressurized vessel to a hydrogen captive plasma generated by a constant current W electrode set. The structural makeup of the hydride ion is that of a *1s1s'* orbital structure with two orthogonal *s*-orbitals, where the *1s'* is more loosely held [15]. The innate ability of the hydride ion to donate its *1s'* electron allows for its integral role in biochemical reactions and facilitates its use as a biochemical "fuel cell." Recent publications on silica hydride have shown the compound to be nontoxic and safe for consumption [16–18]. Some of the unique characteristics of the compound include its abilities: (i) to allow a stable release of the hydride ion in an aqueous environment for an extended length of time, (ii) to act as an effective antioxidant, (iii) for the in vitro reduction of NAD^+ to NADH, (iv) in the moderation of the in vivo reduction of lactic acid production after exercise, and (v) to create an increase in vitro in ATP production in mitochondria [19–21].

The addition of silica hydride to water significantly reduces the potential up to −850 mV as measured by ORP. Because ORP alone is not indicative of the true reducing power of a compound due to proton interactions from changes in pH [22], a variation of the Nernst equation (Eqn. 1) proves to be an effective means to measure the reducing potential for a compound that is reported in units of rH, a logarithmic scaled report denoting absolute reducing potential.

$$E_h = 1.23 - \frac{RT}{F}\,pH - \frac{RT}{4F}\ln\frac{1}{P_o} \qquad (1)$$

Where E_h is the measured oxidation-reduction potential, F is the Faraday constant, R is the universal gas constant, and T is absolute temperature. The value of 1.23 accounts for potential of oxygen under one atmosphere being 1.23 V greater than in a solution of the same pH. rH is defined explicitly as the negative logarithm of the oxygen pressure, P_o (Eqn. 2).

$$rH = -\log P_o \qquad (2)$$

Silica hydride has been shown to have an rH value of 10, indicating its ability to be a more effective reducing agent than other compounds. Comparatively, silica hydride maintains a greater reducing potential than vitamin C (rH 23), ubiquinone (rH 19), and beta-carotene (rH 26).

In addition to inducing a significant change in ORP, silica hydride raises the pH of a solution alkaline to about 8.7. This combination of reduction potential and pH makes for an incredible reducing agent, allowing it to assume numerous roles as an antioxidant and radical scavenger. Some studies have reported results indicating that the pH of the solution has a significant impact on the efficacy of the antioxidant. An alkaline solution at about pH 8.5 has been shown to overtly increase the antioxidant effect by up to 60% relative to the same compound tested in a near biological pH of 7.4 [23].

The use of cell photosensitization has been well established and utilized in the analysis of cellular toxicity, antioxidants, and chemotherapeutic agents, in addition to the in vivo and in vitro diagnosis and treatment of physical disorders [24–26]. Traditionally, antioxidant studies have employed agents such as 2,2′-azobis-2-amidinopropane hydrochloride (AAPH) or cyanide-containing compounds like sulfonated Zn-phthalocyanine and merocyanine 540 to photosensitize plasma membranes [27–29]. The specificity in chemical induction, reaction rates, and the ease of controlling photosensitiz-

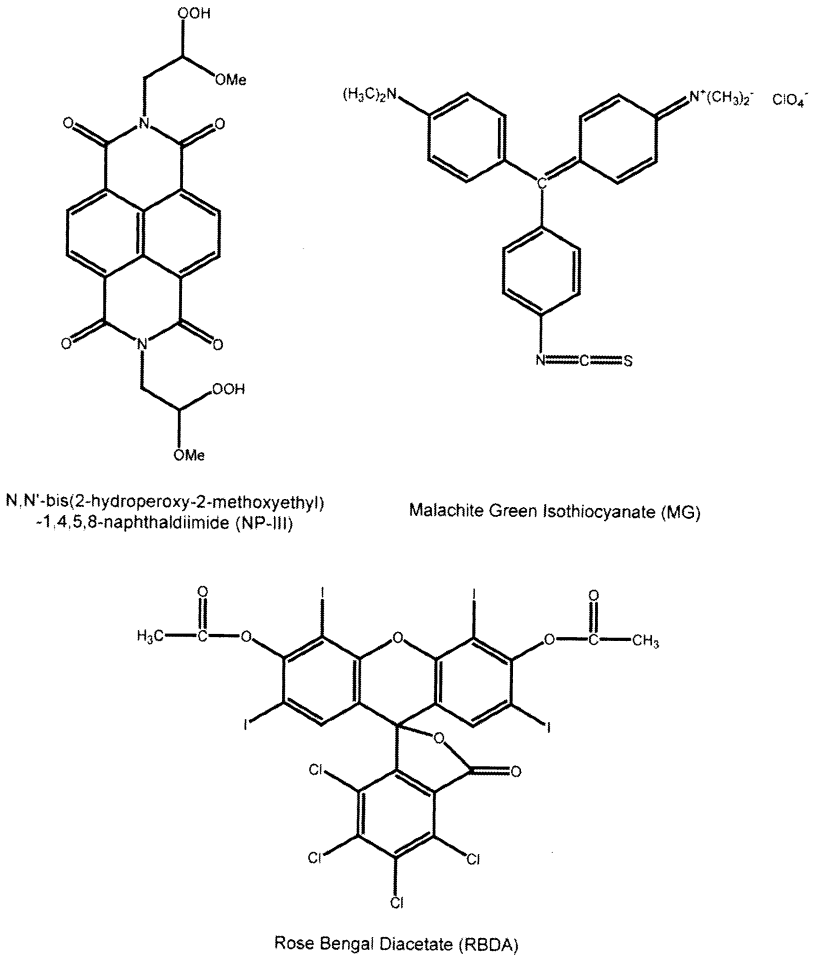

Fig. 2. The photosensitizers used in this analysis. N,N′-bis(2-hydroperoxy-2-methoxyethyl)-1,4,5,8-naphthaldiimide (NP-III), also known as a photo-Fenton reagent, produces near quantitative hydroxyl radicals. Malachite Green isothiocyanate (MG) produces a mixture of superoxide anions and hydroxyl radicals when excited. Rose Bengal diacetate (RBDA) produces near quantitative amounts of singlet oxygen ROS.

ers offers a convenient model allowing for both the quantitative and qualitative analysis of reducing agents as antioxidant scavengers [29–33].

Three photosensitizing compounds, rose Bengal diacetate (RBDA), malachite green isothiocyanate (MG), and N,N′-bis(2-hydroperoxy-2-methoxyethyl)-1,4,5,8-naphthaldiimide (NP-III), known as the photo-Fenton reagent, were used to introduce singlet oxygen, hydroxyl/superoxide ROS, and hydroxyl radicals, respectively [34–38]. Each photosensitizer used is detailed in Fig. 2. RBDA utilizes a Type-II photochemical pathway where the excited photosensitizer reacts with molecular O_2 to form singlet oxygen. MG functions in a Type-I photochemical pathway by transferring a hydrogen or electron to form the oxygenated products of hydroxyl and superoxide ROS, respectively. The NP-III Type-I mechanism directly transfers the hydrogen to produce quantitative hydroxyl radicals in a 2:1 stoichiometric fashion. Figure 3 demonstrates the Type-I and -II mechanisms of the photosensitizers used in this analysis.

The quantification of cell viability is determined through the use of the esterase and nucleic acid intercollating dyes, calcein AM, and ethidium homodimer-1 (EthD-1) [39–41]. This experiment involves separately introducing several types of common, biologically significant radicals into Chinese Hamster Ovary (CHO) and Mouse Hybridoma (NS-1) cells, photosensitizing them to invoke cytotoxicity, and then checking for cell viability and toxicity by using fluorescent probes designed to detect esterase activity in cellular membranes. The results objectively characterized the cell as viable or cytotoxic. Each photosensitized cell line, both having been treated and nontreated with silica hydride, was analyzed for cytotoxicity. The fluorescence signals of the fluorophores are monitored at 530 nm, as summarized by the following reaction scheme (Eqn. 3):

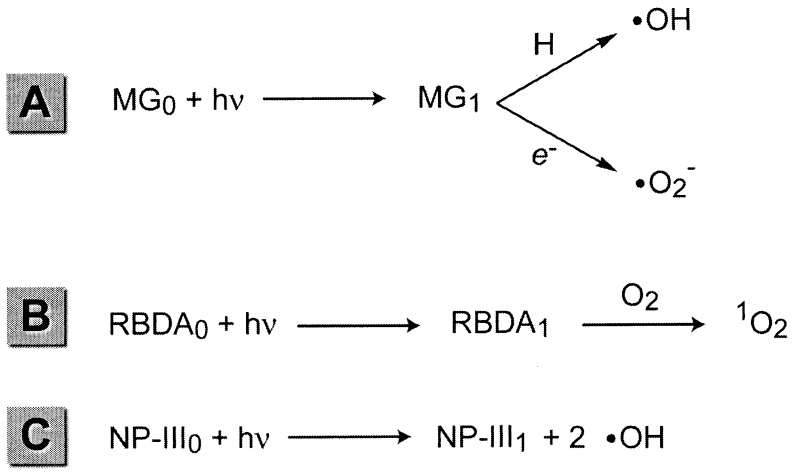

Fig. 3. The photochemical mechanisms of the photosensitizers. The Type-I photochemical mechanism malachite green (A), stimulates the ground-state, MG_0 with 632 nm light producing the excited state, MG_1, which transfers a hydrogen or an electron, producing hydroxyl radicals or superoxide ROS, respectively. (B) The rose Bengal ground-state, $RBDA_0$, is excited as a Type-II mechanism by 543 nm light producing $RBDA_1$, which further binds with molecular oxygen to produce singlet oxygen ROS. (C) The ground-state N,N′-bis(2-hydroperoxy-2-methoxyethyl)-1,4,5,8-naphthaldiimide, $NP\text{-}III_0$, is excited as a Type-I mechanism to $NP\text{-}III_1$ at 355 nm to directly transfer a hydrogen to produce hydroxyl radicals.

$$\text{sensitizer} + \text{cells} \xrightarrow[\text{EthD-1}]{\text{Calcein AM}}$$

$$h\nu + SH \rightarrow \begin{matrix}\text{fluorscence detection} \\ \text{485 nm ex/530 nm em}\end{matrix} \quad (3)$$

Where the unexcited sensitizer is combined with live cells and intercollating viability stains (Calcein AM and EthD-1), then excited with laser light in the presence of a potential antioxidant, in this case, silica hydride (SH). The results are quantified by monitoring the emitted fluorescence.

Using animal cells as a human biological model, this study objectively and quantitatively illustrates the in vitro antioxidant properties of silica hydride through the introduction of the novel combinational technique of using both photosensitizers and viability probes for ROS analyses.

MATERIALS AND METHODS

Chemicals

The photosensitizers, rose bengal diacetate (RBDA), and malachite green (MG), in addition to the viability and cell toxicity kit containing calcein AM and ethidium homodimer (EthD-1), sold as LIVE/DEAD Kit L-3224, were from Molecular Probes (Eugene, OR, USA). Unless otherwise noted, all other reagents were from Sigma-Aldrich (St. Louis, MO, USA).

Cell preparation

CHO and NS-1 cells (7.0 ml each) were incubated at 37° while the reagents from the proceeding section were prepared. Each cell line sample was centrifuged at 100 × *g* and the supernatant removed, then washed twice with a 50 mM potassium phosphate (pH 7.4) buffer. The final centrifuged pellets of each cell line were suspended in 3.0 ml of buffer. Seven aliquots of 1.0 ml each, for both cell lines, were pipetted into 2.0 ml centrifuge tubes. Twenty microliters of solution was placed on a hemocytometer and determined to be 3×10^4 cells/ml.

Singlet oxygen ROS introduction

Under UV lighting, a 4 μM solution of RBDA was made in DMSO; 1.0 ml of the RBDA solution was added to two of each of the previously prepared 1.0 ml aliquots of both NS-1 and CHO cells. The cells were allowed to stain at 23° for 45 min. The stained cells were washed twice with 50 mM potassium phosphate buffer.

Hydroxyl and superoxide ROS introduction

Under UV lighting, a 4 μM solution of MG was made in DMSO and prepared using both cell lines as described for the *singlet oxygen introduction.*

Hydroxyl radical introduction

A 2 μM solution of NP-III was synthesized from naphthalene-1,4,5,8-tetracarboxylic anhydride, 2,2-dimethoxyethylamine in dichloromethane, and ethereal hydrogen peroxide, as previously described [38], and pre-

pared using both cell lines as described for the *singlet oxygen introduction*.

Cell viability and cytotoxicity staining

To add the fluorescent viability probes to the cell lines, each of the four RBDA, NP-III, and MG suspensions for both NS-1 and CHO cells were centrifuged at 100 × *g* and the supernatant removed. The LIVE/DEAD mixture, consisting of 1.0 ml of a 2 μM calcein AM and 4 μM EthD-1 solution was prepared by the following: 20 μl of the supplied stock EthD-1 solution was added to 10.0 ml 50 mM PBS/50 mM KH_2PO_4 (pH 7.4). The working solution was added to the cell pellets and vortexed to ensure mixing, and then 5 μl of calcein AM stock supplied stock solution was added and further vortexed. The solution was allowed to stain each of the cells for 30 min at 23°.

Control preparation

As a control, two 1.0 ml aliquots of each of the original cell suspensions were stained with the LIVE/DEAD mixture as previously described. These, however, were not photosensitized. Additional noncellular controls to substantiate that the silica hydride was not affecting the fluorescence excitation or emission were also prepared. One milliliter of 500 μg/ml aliquots of aqueous solutions of silica hydride prepared in ddH_2O were combined with 1 ml solutions of 4 μM RBDA, 2 μM NP-III, and 4 μM MG. Similar controls were prepared and tested spectrafluorometrically with the LIVE/DEAD calcein AM/EthD-1 mixture.

Silica hydride preparation

Five hundred microgram aliquots of silica hydride were prepared as previously described [14] and were added to one sample of RBDA stained cells, MG stained cells, NP-III stained cells, and one control vial for both NS-1 and CHO cells, then vortexed for 30 s.

Experimental

Upon the completion of the prepared cell suspensions, 150 μl of each of the samples were placed into 150 μl sample quartz cuvettes. All of the RBDA-stained samples were sensitized by treatment with the 543 nm spectral line of a KrAr laser (Model 171, Spectra Physics, Fremont, CA, USA) for 30 min at 1500 W/m^2. All samples of MG-stained cells were sensitized by treatment with the 632 nm line of a KrAr laser (Model 171, Spectra Physics) for 30 min at 2000 W/m^2. All of the NP-III stained samples were sensitized by treatment with a linear-variable-filter selected 355 nm ± 10 nm UV line of a broadband photometric excitation system (Model DT1000, Analytical Systems, Inc., Dunedin, FL, USA) for 30 min at 1250 W/m^2.

Table 1. Overview of the Experimental Parameters for the Analysis

Experiment	Cell type	Sensitizer	ROS	Silica hydride treated	Laser/ time (min)
1	NS-1*	None	N/A	No	
2	NS-1	RBDA	$^1O_2$	Yes	543.5/30
3	NS-1	RBDA	$^1O_2$	No	543.5/30
4	NS-1	MG	$O_2^{\bullet -}$/$^{\bullet}OH$	Yes	632.8/30
5	NS-1	MG	$O_2^{\bullet -}$/$^{\bullet}OH$	No	632.8/30
6	NS-1	NP-III	OH	Yes	355/30
7	NS-1	NP-III	OH	No	355/30
8	CHO*	None	N/A	No	
9	CHO	RBDA	$^1O_2$	Yes	543.5/30
10	CHO	RBDA	$^1O_2$	No	543.5/30
11	CHO	MG	$O_2^{\bullet -}$/$^{\bullet}OH$	Yes	632.8/30
12	CHO	MG	$O_2^{\bullet -}$/$^{\bullet}OH$	No	632.8/30
13	CHO	NP-III	OH	Yes	355/30
14	CHO	NP-III	OH	No	355/30

* denotes control.

Each of the samples were analyzed by a spectrafluorometer (FP-750, Jasco, Inc., Eaton, MD, USA) at 485 nm excitation and 530 nm emission, then viewed by fluorescence microscopy using an XF25 long pass filter (Omega Optical, Brattleboro, VT, USA). Spectra were taken and recorded to calculate the percent viability. Each assay was performed in six replicates. The experimental details are summarized in Table 1.

RESULTS

For the control analysis, the excitation and emission spectra of both working solutions remained the same as the spectra of the stock solutions of RBDA, NP-III, and MG. The results showed no statistical difference in the excitation or emission spectra.

The mechanism of the method involves the nonfluorescent and cell-permeant calcein AM reacting with intracellular esterase to create a vibrantly fluorescent polyanionic calcein (530 nm em.), which is readily retained by live cells producing the esterase. Should the integrity of the cell membrane become compromised through photosensitization cytotoxicity of the reactive oxygen species, the EthD-1 enters the cell and esterase activity ceases, quenching the calcein emission and revealing the now fluorescent EthD-1 (645 nm em.) bound to nucleic acids [42]. The absolute number of living cells is linearly related to the fluorescence signal obtained and the percentage of live cells can be calculated by evaluating the quotient of the difference between the sample and the maximum fluorescence as illustrated by Eqn. 4:

$$\%\ \text{Live Cells} = \frac{F(530)_{sam} - F(530)_{min}}{F(530)_{max} - F(530)_{min}} \times 100\% \qquad (4)$$

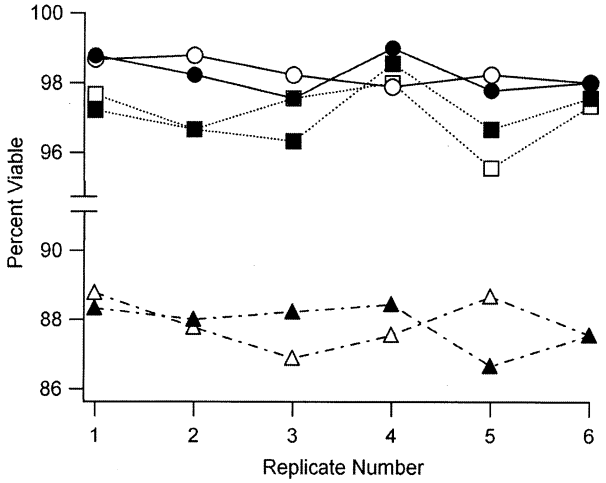

Fig. 4. Chart of the percent viability of silica hydride treated NS-1 and CHO cells as determined by calcein AM spectrafluorometric analysis at 530 nm.: (■) NS-1 RBDA, (□) CHO RBDA, (▲) NS-1 MG, (△)CHO MG, (●) NS-1 NP-III, and (○) CHO NP-III assays were performed in six replicates with consistent overall results, 87.9% (± 0.56%, σ = 0.70) for MG, 97.1% (± 0.68%, σ = 0.84) for RBDA and 98.2% (± 0.37%, σ = 0.47) for NP-III, cumulatively, for both cell types.

Where the fluorescence background noise, $F(530)_{min}$ is subtracted from the sample reading, $F(530)_{sam}$, and the maximum fluorescence reading, $F(530)_{max}$. Reference spectra were taken of the stock calcein/EthD-1 solution to get a maximum fluorescence reading. Additional reference spectra were taken of the PBS/KH_2PO_4 buffer to obtain a background reading for the spectrafluorometer.

The data obtained were calculated as a function of percent live cells. The results derived from the fluorometric analysis show a 97.1% cell viability through the reduction of singlet oxygen ROS through the RBDA analysis, an 87.9% cell viability reduction of the MG produced hydroxyl and superoxide radicals and a 98.2% cell viability through the reduction of hydroxyl radicals through the NP-III analysis. Figure 4 illustrates the viability after photosensitization of treated NS-1 and CHO cell lines being introduced to singlet oxygen radicals (RBDA), hydroxyl/superoxide radicals (MG), and hydroxyl radicals (NP-III).

The viability rate of the nontreated photosensitized cells were 0.57% as illustrated in Fig. 5, demonstrating that the cytotoxicity rates were consistent for RBDA, NP-III, and MG photosensitization techniques on both cell lines.

The controls cumulatively had a survival rate of 99.3% for the CHO cells and 99.2% for the NS-1 cells. Overall, the control survival rate was 99.3% for both cell lines with a standard deviation of 0.6 showing a consistent survival rate for both cell lines. The overall data for the experiment are shown in Table 2.

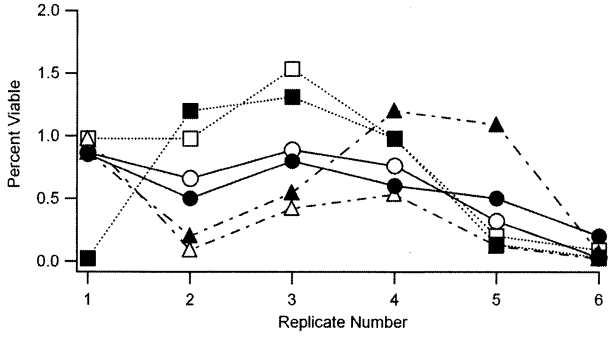

Fig. 5. Chart of percent viability of the photosensitized, but nontreated CHO and NS-1 cells. The representation of the cells are as follows: (■) NS-1 RBDA, (□) CHO RBDA, (▲) NS-1 MG, (△) CHO MG, (●) NS-1 NP-III, and (○) CHO NP-III. The overall viability statistics for RBDA, MG, and NP-III, respectively, are 0.70% ± 0.46% (σ = 0.45), 0.51% ± 0.31% (σ = 0.40) and 0.50% ± 0.41% (σ = 0.55).

DISCUSSION

The use of this novel combinational method offers an easy and consistent method of radical scavenging analysis. Its use could be extrapolated to utilize other photosensitizing compounds to introduce the ROS into the cell lines.

The use of silica hydride as a radical scavenger and antioxidant seem very promising with this in vitro analysis. The data provide significant evidence that the compound, silica hydride, is able to efficiently reduce the radicals introduced into the cell lines. The efficacy of the compound against singlet oxygen ROS seems to be the greatest with less than a 2.5% loss of cell viability as compared with the controls, which averaged 99.26% (σ = 0.6) for both cell lines combined. The effectiveness against the combined hydroxyl and superoxide radicals occurs with about a 12% loss, and data from the pure hydroxyl radicals indicate just greater than a 1% loss compared to the same controls. Interestingly, the difference between the RBDA, NP-III, and the MG assays were not as expected with the MG results much lower than the kinetics of the electron abstraction capacity of a hydroxyl radical and superoxide ROS, would elude to. Perhaps the nonspecificity of the MG creating both hydroxyl radicals ($k \sim 5 \times 10^9$ $M^{-1}s^{-1}$) and superoxide ROS ($k \sim 9 \times 10^7$ $M^{-1}s^{-1}$) accounts for these differences, particularly when considering the Type-I mechanism decay pathway of MG. Within this mechanism, several mechanics are simultaneously occurring that may bias this result. First, the ionization and formation of peroxide by the hydroxyl radical, as well as the direct attack by the radical species on the experimental buffer, may account for a primary or secondary reactivity with the PBS buffer used in this analysis. Additionally, the dismutation of the superoxide anion to peroxide and molecular oxygen has a significantly slower rate ($k_2 \sim 5$

Table 2. Results of the Photosensitization Assay for the Analysis of ROS Reduction by the Silica Hydride Compound

Experiment	Cell type/agent	Treated	Percent viable (Ave %)	St. Dev	+/− %
1	NS-1*		99.24	0.68	0.54
2	NS-1/RBDA	Yes	97.16	0.81	0.64
3	NS-1/RBDA	No	0.61	0.61	0.49
4	NS-1/MG	Yes	87.87	0.67	0.53
5	NS-1/MG	No	0.66	0.46	0.37
6	NS-1/NP-III	Yes	98.22	0.57	0.45
7	NS-1/NP-III	No	0.34	0.32	0.26
8	CHO*		99.31	0.64	0.52
9	CHO/RBDA	Yes	97.12	.89	0.71
10	CHO/RBDA	No	0.79	0.55	0.44
11	CHO/MG	Yes	87.87	0.73	0.58
12	CHO/MG	No	0.36	0.35	0.29
13	CHO/NP-III	Yes	98.30	0.36	0.28
14	CHO/NP-III	No	0.66	0.47	0.37

* denotes control.

$\times 10^4$ $M^{-1}s^{-1}$) when in a localized alkaline environment, as in the case in this analysis. Also, the superoxide anion itself may act as a reducing agent and bias the reactivity of the hydroxyl radicals formed. The efficiency of the silica hydride to reduce each of the different radical types did not significantly vary between cell lines, providing a basis to further hypothesize about the efficacy on all cell types. NS-1 and CHO are reliable indicators of how a compound may affect a human system [43–45]. Additionally, the silica hydride performed well in the reduction and elimination of ROS and in cellular protection from oxidative stress.

This cost effective, simple, but informative assay not only evaluated the ability of silica hydride to act as an antioxidant, but also introduced the combinational techniques of using spectrafluorometry with photosensitization to quantify the antioxidant properties of biological reducing agents. This particular analysis utilized the calcein fluorescence in intact cells to obtain a percent viability. Additionally, these same techniques used in this analysis may be used to calculate a percent dead/cytotoxic by evaluating the fluorescence at 645 nm. Once cellular esterase activity ceases in a cytotoxic cell, the ethidium homodimer-1 binds with nucleic acids and fluoresces a vibrant red. Because the viability probes also have absorbance and transmittance properties, this technique would also accommodate the testing of multiple ROS types by a photometric analysis. The photosensitization assays performed provide significant evidence that silica hydride is an effective tool in the reduction of free radicals.

To validate the results obtained by this novel method and to aid in understanding silica hydride's role in the MG analysis, additional tests were performed by outside sources to confirm the in-house, fluorometric results. Three traditional analyses were performed. Spectrophotometric analyses [46] indicate an increase in the NADH/NAD^+ ratio, in addition to an increase in mitochondrial membrane potential ($\Delta\Psi$). The cumulative results indicate the neutralizations of radical species, presumably by the 1s' electron donation from the hydride ion in solution within the siliceous silsesquioxane cage of the silica hydride.

The compound was shown to specifically reduce Fe(III) cytochrome c to Fe(II) cytochrome c (Eqn. 5) and NAD^+ to NADH (Eqn. 6) [47]:

$$\text{Silica}(H^-) + \text{cyt c}(Fe^{+3}) \rightarrow \text{Silica} + \text{cyt c}(Fe^{+2}) + H^+ \quad (5)$$

$$\text{Silica}(H^-) + NAD^+ \rightarrow \text{Silica} + \text{NADH} \quad (6)$$

Additionally, the analysis showed the reduction of cytochrome *c* by superoxide was inhibited (Eqn. 7), indicating that the superoxide radical was reduced.

$$O_2^{\bullet -} + \text{cyt c}(Fe^{+3}) \rightarrow O_2 + \text{cyt c}(Fe^{+2}) \quad (7)$$

Because silica hydride reduced both the Fe(III) cytochrome *c* in and inhibited the superoxide/cytochrome *c* reduction, an additional assay was performed to clear up any confusion about its role in radical reactions. The second assay observed the oxidation of epinephrine to adenochrome by superoxide (Eqn. 8):

$$O_2^{\bullet -} + \text{epinephrine} \rightarrow H_2O_2 + \text{adrenochrome} \quad (8)$$

Upon the addition of silica hydride, the superoxide was scavenged, leaving epinephrine, illustrating the antioxidant activity of the compound.

An additional control assay was performed using ESR spectroscopy to measure hydroxyl radical reduction [48]. The conclusion of the assay was that silica hydride

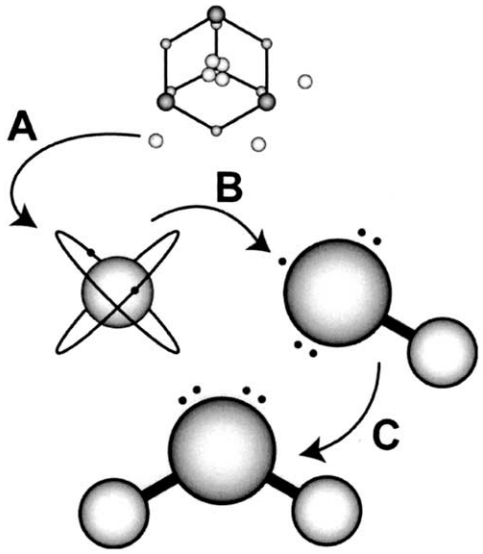

Fig. 6. In an aqueous solution, the interstitially embedded hydride anions dissociate (A) into the solution where the 1 s' electron of the anion is donated (B) to the unpaired electron of the radical species, in this example, the hydroxyl radical. The product of this reaction (C) produces water from the neutralized postradical species.

demonstrates antioxidant activity towards hydroxyl radicals and ROS, in general, where the mechanism follows the electron rich, 1s1s' orbital [15] of the hydride anion reacting with the electron deficient radical as depicted mechanistically in Fig. 6. The results obtained by the supplementary assays are consistent with the results of additional experimentation and indicate that the potential for the compound to be an effective antioxidant is quite high.

This article proposes that the use of silica hydride may significantly reduce the oxidative stress and resultant pathologies induced by ROS in an efficient and effective manner. This is objectively illustrated by the introduction of the novel combinational technique of utilizing fluorescent adducts depicting cellular viability and the integration with photosensitizer-induced oxidative stress and reactive species incorporation.

Acknowledgements — A special thank you to J. J. Lemasters at University of North Carolina at Chapel Hill, J. M. McCord at the Webb-Waring Institute for Cancer, Aging and Antioxidant Research at the University of Colorado Health Sciences Center, and L. Packer at the University of California, Berkley for their respective participation in the antioxidant analysis of the silicate mineral compound.

REFERENCES

[1] Sies, H. Oxidative stress. New York, London: Academic Press; 1985.
[2] Ji, L. L. Oxidative stress and antioxidant response during exercise. *Free Radic. Biol. Med.* **6:**1079–1086; 1995.
[3] Beckman, J. S.; Beckman, T. W.; Chen, J.; Marshall, P. A.; Freeman, B. A. Apparent hydroxyl radical production by peroxynitrite: implications for endothelial injury from nitric oxide and superoxide. *Proc. Natl. Acad. Sci. USA* **87:**1620–1624; 1990.
[4] Grune, T.; Klotz, L.; Gieche, J.; Rudeck, M.; Sies, H. Protein oxidation and proteolysis by the nonradical oxidants singlet oxygen or peroxynitrite. *Free Radic. Biol. Med.* **30:**1243–1253; 2001.
[5] Dean, R. T.; Fu, S.; Stocker, R.; Davies, M. J. Biochemistry and pathology of radical mediated protein oxidation. *Biochem. J.* **324:**1–18; 1997.
[6] Halliwell, B.; Gutteridge, J. M. C. Chemistry of free radicals and related reactive species. In: *Free radicals in biology and medicine*, 3rd ed. Oxford, UK: Clarendon Press; 1996:36–107.
[7] Balentine, J. Pathology of oxygen toxicity. New York, London: Academic Press; 1982.
[8] Halliwell, B.; Gutteridge, J. M. C.; Cross, C. E. Free radicals, antioxidants, and human disease: where are we now? *J. Lab. Clin. Med.* **119:**598–620; 1992.
[9] Grune, T.; Klotz, L.; Gieche, J.; Rudeck, M.; Sies, H. Protein oxidation and proteolysis by the nonradical oxidants singlet oxygen or peroxynitrite. *Free Radic. Biol. Med.* **30:**1243–1253; 2001.
[10] Pattanayak, D.; Chatterjee, S. R. Inactivation of sunflower NADH: nitrate reductase by white light-activated rose bengal. *Mol. Cell. Biol. Commun.* **138:**237–240; 1999.
[11] Kim, A. T.; Sarafian, T. A.; Shau, H. Characterization of antioxidant properties of natural killer-enhancing factor-b and induction of its expression by hydrogen peroxide. *Toxicol. Appl. Pharmacol.* **147:**124–128; 1997.
[12] Rosen, G. M.; Cohen, M. S.; Britigan, B. E.; Pou, S. Application of spin traps to biological systems. *Free Radic. Res. Commun.* **9:**187–195; 1990.
[13] Yang, X. F.; Guo, X. Q. Fe(II)-EDTA chelate-induced aromatic hydroxylation of terephthalate as a new method for the evaluation of hydroxyl radical-scavenging ability. *Analyst* **126:**928–932; 2001.
[14] Stephanson, C. J.; Flanagan, G. P. Synthesis of a novel anionic hydride organosiloxane presenting biochemical properties. *Int. J. Hydrogen Energy* **28**(11):1243–1250; 2003.
[15] Gauyacq, J. Dynamics of negative ions. *World scientific lecture notes in physics, vol. 15.* River Edge, NJ: World Scientific Press; 1987.
[16] Flanagan, G. P.; Purdy-Loyd, K. A silicate mineral supplement, Microhydrin traps reduced hydrogen providing *in vitro* biological antioxidant properties. *Proc. Natl. Hydrogen Assoc.* **10:**595–610; 1999.
[17] Carlisle, E. M. The nutritional essentiality of silicon. *Nutr. Rev.* **40:**193–197; 1982.
[18] Keller, W. D.; Feder, G. L. Chemical analysis of water used in Hunza, Pakistan. In: *Trace substances in environmental health-XIII, Proceedings*. Columbia, MO: University of Missouri-Columbia; 1979:130–137.
[19] Stephanson, C. J.; Flanagan, G. P. Evaluation of hydroxyl radical-scavenging abilities of silica hydride, an antioxidant compound, by a Fe+2-EDTA induced 2-hydroxyterephthalate fluorometric analysis. *J. Med. Food* **6**(3):18–21; 2003.
[20] Stephanson, C. J.; Flanagan G. P. Non-toxic hydride energy source for biochemical and industrial venues: ORP and NAD^+ reduction analyses. *Int. J. Hydrogen Energy* In press; 2003.
[21] Purdy-Lloyd, K. L.; Wasmund, W.; Smith, L.; Raven, P. B. Clinical effects of a dietary antioxidant silicate supplement, Microhydrin, on cardiovascular response to exercise. *J. Med. Food* **4:**153–161; 2001.
[22] Clark, M.; Cohen, B. Studies of oxidation-reduction: II. An analysis of the relations between reduction potential and pH. *Public Health Rep.* **38:**666–683; 1923.
[23] Lee, H.; Cha, M.; Kim, I. Activation of thiol-dependant antioxidant activity of human serum albumin by alkaline pH is due to the b-like conformational change. *Arch. Biochem. Biophys.* **380:**308–318; 2000.
[24] Afkhami, A.; Rezaei, M. Sensitive spectrophotometric determi-

nation of formaldehyde by inhibition of the malachite green-sulfite reaction. *Microchem. J.* **63:**243–249; 1999.

[25] Smolen, J. E.; Petersen, T. K.; Koch, C.; O'Keefe, S. J.; Hanlon, W. A.; Seo, S.; Pearson, D.; Fossett, M. C.; Simon, S. I. L-selectin signaling of neutrophil adhesion and degranulation involves p38 mitogen-activated protein kinase. *J. Biol. Chem.* **275:**15876–15884; 2000.

[26] Regoli, F.; Winston, G. W. Quantification of total oxidant scavenging capacity of antioxidants for peronitrite, peroxyl radicals, and hydroxyl radicals. *Toxicol. Appl. Pharmacol.* **156:**96–105; 1999.

[27] Killig, F.; Kunz, L.; Stark, G. Photomodification of the electrical properties of the plasma membrane: a comparison between 6 different membrane-active photosensitizers. *J. Membr. Biol.* **181:** 41–46; 2001.

[28] Yuying, H.; Jingyi, A.; Lijin, J. Glycoconjugated hypocrellin: photosensitized generation of free radicals ($O_2^{\bullet -}$, $^{\bullet}OH$, and $GHB^{\bullet -}$) and singlet oxygen ($^1O_2$). *Free Radic. Biol. Med.* **27:** 203–212; 1999.

[29] Zang, L. Y.; Vankuijk, F. J. G. M.; Misra, B. R.; Misra, H. P. The specificity and product of quenching singlet oxygen by 2,2,6,6-tetramethylpiperidine. *Biochem. Mol. Biol. Int.* **37:**283–293; 1995.

[30] Cao, G.; Alessio, H. M.; Cutler, R. G. Oxygen-radical absorbance capacity assay for antioxidants. *Free Radic. Biol. Med.* **14:**303–311; 1993.

[31] Hirayama, O.; Takagi, M.; Hukumoto, K.; Katoh, S. Evaluation of antioxidant activity by chemiluminescence. *Anal. Biochem.* **247:** 237–241; 1996.

[32] Xue, L.; Chiu, S.; Oleinick, N. L. Photodynamic therapy-induced death of mcf-7 human breast cancer cells: a role for caspase-3 in the late steps of apoptosis but not for the critical lethal event. *Exp. Cell Res.* **263:**145–155; 2001.

[33] Ghiselli, A.; Serafini, M.; Maiani, G.; Azzini, E.; Ferro-Luzzi, A. A fluorescence-based method for measuring total plasma antioxidant capability. *Free Radic. Biol. Med.* **18:**29–36; 1995.

[34] Bottiroli, G.; Croce, A. C.; Balzarini, P.; Locatelli, D.; Baglioni, P.; Lo Nostro, P.; Monici, M.; Patesi, R. Enzyme-assisted cell photosensitization: a proposal for an efficient approach to tumor therapy and diagnosis: the rose Bengal fluorogenic substrate. *Photochem. Photobiol.* **66:**374–383; 1997.

[35] Liao, J. C.; Roider, J.; Jay, D. G. Chromophore-assisted laser inactivation of proteins is mediated by the photogeneration of free radicals. *Proc. Natl. Acad. Sci. USA* **91:**2659–2663; 1994.

[36] Rao, K. V. K.; Mahudawala, D. M.; Redkar, A. A. Malignant transformation of Syrian hamster embryo (SHE) cells in primary culture by malachite green: transformation is associated with abrogation of G2/M checkpoint control. *Cell Biol. Int.* **22:**581–589; 1998.

[37] Valenzeno, D. P.; Tarr, M. CH3 cells, ionic currents and cell killing: photomodification sensitized by rose bengal. *Photochem. Photobiol.* **68:**519–523; 2000.

[38] Guptasarama, P.; Balasubramanian, D.; Matsugo, S.; Saito, I. Hydroxyl radical mediated damage to proteins, with special reference to crystallins. *Biochemistry* **31:**4296–4303; 1992.

[39] Read, T. A.; Sorensen, D. R.; Mahesparan, R.; Enger, P. O.; Timpe, R.; Olsen, B. R.; Hjelstuen, M. H.; Haraldseth, O.; Bjerkvig, R. Local endostatin treatment of gliomas administered by microencapsulated producer cells. *Nat. Biotechnol.* **19:**29–34; 2001.

[40] Gobbel, G. T.; Chan, P. H. Neuronal death is an active, capase-dependant process after moderate but not severe DNA damage. *J. Neurochem.* **76:**520–531; 2001.

[41] Hodder, P. S.; Beeson, C.; Ruzicka, J. Equilibrium and kinetic measurements of muscarinic receptor antagonism on living cells using bead injection spectroscopy. *Anal. Chem.* **72:**3109–3115; 2000.

[42] Hayes, A. W, ed. *Principles and methods of toxicology*, 3rd ed. New York: Raven Press; 1994.

[43] Rapp, S.; Soto, U.; Just, W. W. Import of firefly luciferase into peroxisomes of permeabilized Chinese hamster ovary cells: a model system to study peroxisomal protein import in vitro. *Exp. Cell Res.* **205:**59–65; 1993.

[44] Morse, H. C. III; Tidmarsh, G. F.; Holmes, K. L.; Frederickson, T. F.; Hartley, J. N.; Pierce, J. H.; Langdon, W. Y.; Dailey, M. O.; Weissman, I. L. Expression of the 6C3 antigen on murine hematopoietic neoplasms. Association with expression of abl, ras, fes, src, erbB, and Cas NS-1 oncogenes but not with myc. *J. Exp. Med.* **165:**920–925; 1987.

[45] Bogen, K. T.; Weinfeld, M.; Le, X. C.; Murtha, A. D.; Langlois, R.; Keating, G. DNA Damage vs. Cell Killing by Low-Dose-Rate Gamma Radiation Ultrasensitive Measures and Implications for Mechanistically Modeled Cancer Risk. *DOE Low Dose Radiation: Research Program Workshop I.* November 10–12, Washington, D.C.; abstr.; 1999.

[46] LeMasters, J. J. Spectrophotometric analysis of mitochondrial NAD^+/NADH ratios and membrane potential. University of North Carolina, Chapel Hill; personal communication, 2000.

[47] McCord, J. M. *Cytochrome* C and NAD^+ reduction analyses of silica hydride. Webb-Waring Institute for Cancer, Aging and Antioxidant Research at the University of Colorado Health Sciences Center; personal communication, 2000.

[48] Packer, L. ESR analysis of silica hydride on hydroxyl ROS. University of California, Berkley; personal communication, 2000.